Acoustics properties and applications, in Metallic Foams: Fundamentals and Applications

Camille Perrot, F. Chevillotte, L. Jaouen, M. T. Hoang

Chapter 4: Acoustic Properties and Applications

By Camille Perrot [(a)], Fabien Chevillotte [(b)], Luc Jaouen [(b)], and Minh Tan Hoang [(a)]

In NEW BOOK ON METAL FOAM

Metallic Foams: Fundamentals and Applications

Edited by: Nihad Dukhan, Ph.D.

Authors affiliations:

(1) *Université Paris-Est, Laboratoire Modélisation et Simulation Multi Echelle, MSME UMR 8208 CNRS, 5 bd Descartes, 77454 Marne-la-Vallée, France*

(2) *Matelys - Acoustique & Vibrations, 1 rue Baumer, F-69120 Vaulx-en-Velin, France*

Outline

I. Introduction

A major issue in automobile, aeronautical, and building industries concerns the need to increase or adapt the sound absorption spectrum of metallic foams. However, semi-phenomenological models used to characterize and predict sound absorbing material performances are mainly based on interdependent macroscopic parameters, which do not account explicitly for the local geometry of these porous media (i.e., their microstructure). Thus, optimizing sound absorbing materials from the manufacturing step remains a difficult task mostly done by trial and error. A strict optimization method would firstly rely on our ability to predict the acoustic properties of real metallic foam samples from the description of their local geometry. Secondly, it would propose process-compatible modifications of their microstructure having predictable impacts on their absorption spectrum. Based on fundamental mechanisms governing audible sound waves propagation and dissipation through metallic foams, emphasis of this chapter is on linking scales in computational acoustics of porous media: how microstructure and macro-scale properties of real metal foam samples are related, with engineering guidelines for sound proofing.

What is the influence of the micro-structural morphology (e. g. aperture size, pore size, ligament diameter, ligament shape, etc.) of a metallic foam on its acoustical performance? What can be done to the foam's structure to make it a better absorber? These are many questions that are dominating studies of relationships between microstructure and acoustic properties of metallic foams. Such questions may be addressed in different manners.

(1) A common method consists in conducting a lot of laboratory measurements on samples of varying microstructural parameters [1-5].

(2) Alternatively, in a search for a theoretical understanding, one may try to better understand the mathematical and physical basis of the macroscopic equations governing acoustic dissipation phenomena [6-15].

(3) Numerical studies based on simulations can be considered [16-24].

(4) Semi-empirical approaches that combine numerical predictions of key physical parameters used as input data in empirical models can be employed [25].

(5) Lastly, one can consider hybrid numerical approaches combing numerical predictions of key physical parameters used as input data in theoretical models [26-29].

Each of these ways of considering these questions has advantages and drawbacks.

(1) Laboratory measurements are of indisputable value; however, their interpretation may be limited to a specific group of morphologies (e.g. open-cell, cracked closed-cell, perforated closed-cell, etc.).

(2) Theoretical studies at the macroscopic scale lead to robust semi-phenomenological models; but they also require measurements of macroscopic parameters, and this may involve great expense.

(3) Numerical simulations usually attempt to bridge the gap between theory and experiments. They are nevertheless typically restrained by either the need to simplify the geometry, physics, or both.

(4) Semi-empirical approaches suffer from the weakness of empirical models providing poor physical insight, and being unable to consider non-already existing microstructural configurations.

(5) In recent years, a hybrid numerical approach to the study of long-wavelength acoustic waves propagation through rigid porous media has gained some popularity. The idea is to numerically solve elementary transport equations in a realistic local geometry model, and then to study how key physical parameters computed from volume-averaged fields, relate to frequency-dependent acoustic properties through approximate but robust semi-phenomonological models. Compared to direct numerical approaches, such studies offer the ability to identify the micro geometry features governing the macro transport and acoustic properties; they are however limited to micro geometries made of idealized periodic unit-cells.

The classical numerical homogenization approach study the long-wavelength acoustic properties of porous media by direct solutions of the linearized Navier-Stokes equation in harmonic regime with the local incompressibility condition [17] (dynamic viscous problem), and of the linearized heat equation in harmonic regime [13] (dynamic thermal problem) with appropriate boundary conditions.

For the case of the dynamic viscous problem, solutions mainly based on finite element methods (FEM) have been investigated. Craggs and Hildebrandt [16] solved the viscous problem for specific cross-sections of uniform pores. Zhou and Sheng [17] treated the case of a cylindrical tube with sinusoidal modulation of its cross section, three-dimensional (3D) fused-spherical-bed and fused-diamond lattices. Chapman and Higdon [18] considered the three cubic lattices [simple cubic (SC), body-centered cubic (BCC), and face-centered cubic (FCC)] from a very accurate semi-analytical method, with overlapping or non-overlapping spheres depending on the prescribed porosity. Firdaouss *et al.* [19] paid attention to a corrugated pore channel. Finite elements results obtained by Firdaouss *et al.* were subsequently confirmed by Cortis and Smeulders using Schwartz-Christoffel transformations [20]. The overall disseminated conclusions related to two-dimensional porous media whose internal surface contains sharp-edged wedges were finally summarized in a clarifying paper [21]. Cortis *et al.* [22] also studied the case of bi-dimensional (2D) configurations made of a square arrangement of solid cylinders.

An attempt to grasp the viscous dynamic behavior of more complex microstructures, such as a real open-cell aluminum foam sample, has been carried out thanks to a basic 2D hexagonal model of solid fibers [24, 26, 30]. The 2D periodic foam model geometry provided a reliable estimate of the dynamic permeability, except in the low frequency range. In the 2D periodic foam model geometry, ligaments are always perpendicular to the flow direction, thus artificially decreasing the static permeability of the viscous flow.

For the case of the dynamic thermal problem, another approach has been the application of the random-walker simulation method, as proposed by Lafarge [31]. The principle of the method consists in simulating Brownian motion for a large number of the fluid-phase particles, and to link their mean square displacements to the thermal conduction properties of the confined fluid. An important point of the method is that, once the mean square displacements of a large number of particles has been estimated, the dynamic thermal response might be obtained for all frequencies. Contrary to finite element analysis, the solution does not need to be computed at each frequency.

The random-walker simulation method has been implemented in two and three dimensions for computing the trapping constant of a 2D arrangement of overlapping fibers of circular cross-sections [32], and 3D digitalized geometries [33]. The trapping constant provides the asymptotic low frequency behavior of the thermal problem. The first numerical simulations in harmonic regime have been achieved for the case of 2D regular and random arrangements of fibers with circular cross-sections [31], and extended to three-dimensional micro geometries [34] with application to an open cell aluminum foam sample [35].

Other contributions at the pore scale, of industrial interest, and which can be applied in order to properly determine both viscous and thermal dissipation phenomena in specific open-cell metallic structures are addressed in this section. Wang and Lu [36] determined the optimized acoustic properties of polygonal ducts through semi-analytical solutions. The optimized cell size found for best sound absorbers is on the order of ~ 0.1 mm for practical combinations of sample thickness, cavity depth, and porosity. Gasser *et al.* [23] treated the 3D case of face centered cubic nickel hollow spheres packings with a view of absorbing sound inside the turboengines of aircraft. A special care was given to properly model solder joints. Alternatively, prescribed porosity and correlation length(s) have been used for the reconstruction process, or three-dimensional images of the real samples [37]. Lee *et al.* paid attention to the three-dimensional hexagonal-closed pack structure which has not appeared in the acoustic literature previously [28]; and showed that multi-periodic composite structures, defined as periodically-layered media wherein each layer is composed of periodic unit-cells, could lead to frequency stop-bands [29]. The sound absorption properties of metallic hollow sphere structures were also analyzed experimentally by Pannert *et al.* [5]. Very recently, membrane, anisotropy, and pore size dispersion effects of real foam samples, mostly open-cell, were investigated by the implementation of a 3D polyhedron unit-cell, a truncated octahedron with ligaments of circular cross-section shapes and spherical nodes at their intersections [38].

Contrary to open-cell foams, closed-cell foams are poor sound absorbers. However, they generally present a better structural rigidity and a lower production cost than open-cell foams. Two main methods can be used for enhancing the sound absorption of closed-cell foams. The first method consists of fracturing its cell walls via compression or rolling [39]. In an effort to model the acoustic properties of such a porous medium, it was shown that the fractured foam may be seen as a semi-open cell material, i.e., a two-dimensional foam model geometry consisting of infinitely long arrays of cracked cells [40]. The second method consists of hole drilling the closed-cell foam [41]. These two methods follow the same principle, which aims at increasing the viscous effects by enabling a relative motion between the two phases of the porous medium. The literature on both methods revealed good practical results; however it was limited in the sense that it did not systematically quantify the effects of microstructure modifications introduced by compression, rolling or hole drilling. Such an attempt was further performed by Chevillotte *et al.* [27].

Let us also mention that sound absorption characteristics of lotus-type porous magnesium and copper plates fabricated by unidirectional solidification were studied experimentally [42]. For the samples under study, it was found that the sound absorption coefficient increased with increasing porosity (43 % to 62 %), while it decreased with increasing pore diameter (from 460 μm to 660 μm).

This chapter is devoted to the hybrid numerical study of long-wavelengths acoustic waves propagation and dissipation through periodically-reconstructed images of rigid porous media. The simulations are performed by a finite element method. Since this chapter is also dedicated to non-specialists, we begin our discussion with a brief review of acoustic wave's dissipation mechanisms in addition to providing some orders of magnitude for typical dissipative pore sizes. We then describe the hybrid numerical method through which we simulate the key physical parameters and acoustical properties of metallic foams. A study of both an open and a perforated closed-cell aluminum foam sample are provided, including a study of how acoustic properties vary as a

function of common local geometry features. Our results compare qualitatively well to laboratory measurements. They thus serve to validate the application of the hybrid numerical method to periodically-reconstructed metallic foams, in addition to providing a detailed study of how acoustic properties vary with morphology.

II. Principles of acoustical energy dissipation through metallic foams

Metallic foams, composed of a metal frame and a connected pore network saturated with air, can be used as passive noise control packages to reduce both structure and air-borne sound and vibrations. The acoustical energy dissipation through such porous media involves 3 phenomena: visco-inertial dissipation, thermal dissipation and structural dissipation.

The visco-inertial dissipation results from the friction of air particles with the metal frame walls while the acoustic waves propagates inside the foam. The thermal dissipation results from the thermal exchanges between the air particles and the frame. These two dissipation phenomena thus depend mainly on the geometry of the pore network. Obviously the structural dissipation depends on the mechanical properties of the material.

Below are further details of these mechanisms of acoustical energy dissipation. A simple physical analysis of these mechanisms will lead to recommendations for producing acoustic absorber foams, to be used as standalone sound packages for acoustic correction purposes, or in association with heavier partition walls for sound insulation purposes.

A large amount of literature is available addressing the dissipation mechanisms of the acoustic energy in porous materials. Readers are invited to refer to the books by Zwikker and Kosten [43] or by Allard and Atalla [44] for example.

A. Mechanisms of acoustical energy dissipation

Porous materials presenting a single scale of porosity such as glass wool or polyurethane foams are constituted by two components called hereafter phases. One phase, the skeleton, is composed by the matter from which the porous medium is made of. The second phase is composed by the fluid saturating the skeleton: air in acoustics. When such diphasic material is submitted to an airborne or a structural vibration, the two phases can interact with each other and can dissipate energy. Three types of interactions can occur: visco-inertial, thermal and structural (if the material's skeleton is deformable).

1. Visco-inertial dissipation mechanisms

Visco-inertial effects in an acoustical porous material are due to the fact that the pore saturating fluid does not move in phase with the skeleton.

In the low frequency range, the viscous forces dominate the inertial ones. The air flow inside the material is described by Darcy law. In the high frequency range, inertial forces dominate the viscous ones. A characteristic angular frequency ω_v has been introduced [6-7, 8] to separate the low and high frequency behaviors of visco-inertial effects. For pulsations much smaller than ω_v the flow is purely viscous, for pulsation much larger than ω_v the flow is purely inertial. See Fig. 1 for a schematic view of these basic principles on visco-inertial dissipation mechanisms.

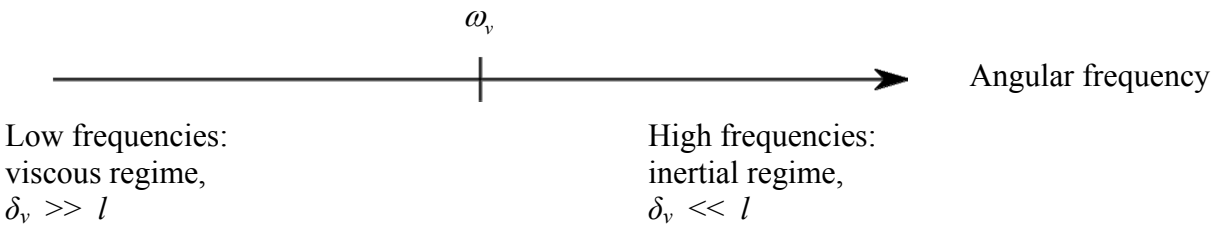

Figure 1. Frequency- dependent visco-inertial dissipation mechanisms

2. Thermal dissipation mechanisms

While a sound wave propagates through a porous medium, it experiences successive compressions and dilatations. During these successive state transformations, a thermal wave is created. Heat is thus exchanged between the air and the frame. The resulting thermal dissipative mechanism follows a similar two-asymptotic-state behavior as the visco-inertial one. Below the thermal characteristic angular frequency ω_t introduced by Lafarge *et al.*[13] the air compressions and dilatations are isothermal (heat exchanges exist between the whole fluid phase and the frame). Above ω_t transformations in the fluid phase can be considered as adiabatic due to the high frequency of the acoustic propagation phenomenon: The heat exchange phenomenon takes longer to establish than a cycle of the pressure wave. See Fig. 2 for a schematic view of these basic principles on thermal dissipation mechanisms.

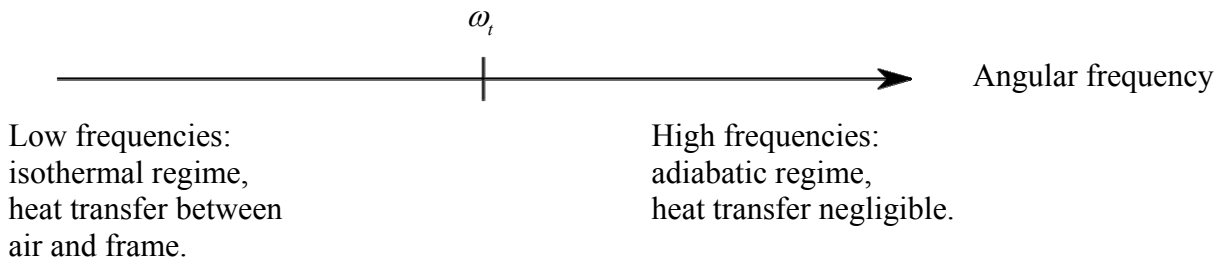

Figure 2. Frequency- dependent thermal dissipation mechanisms

3. Structural dissipation mechanisms

The Biot's theory [6-7] states that in a porous frame saturated by a fluid such as an air-saturated metal foam, three waves can propagate:

1. a longitudinal wave in the air,
2. a longitudinal wave in the frame and,
3. a shear wave in the frame.

Structural dissipation may thus occur in the frame of the metal foam.

In case of air-borne excitation, Zwikker and Kosten [43] introduced an angular frequency ω_{dec} for which the inertial effects in the frame are equal in magnitude to the viscous effects in the fluid phase, Fig. 3. For angular frequencies much larger than ω_{dec} the two phases can be considered as decoupled, assuming stiffness effects of the material sample frame are negligible compared to inertial ones. At such frequencies, the frame cannot be significantly set in motion by the fluid-borne wave having a high frequency, as the frame motion takes longer to establish than a cycle of the pressure wave in the pore network.

Zwikker and Kosten expression of ω_{dec} shows that this angular frequency depends on the pore morphology of the porous medium. ω_{dec} is also inversely proportional to the mass density of the material. For metal foams, the vibration of the frame can usually be neglected as the numerical value of the decoupling angular frequency is in the low part of the audible frequency range. Obviously, for structure-borne sound no phase decoupling can be considered.

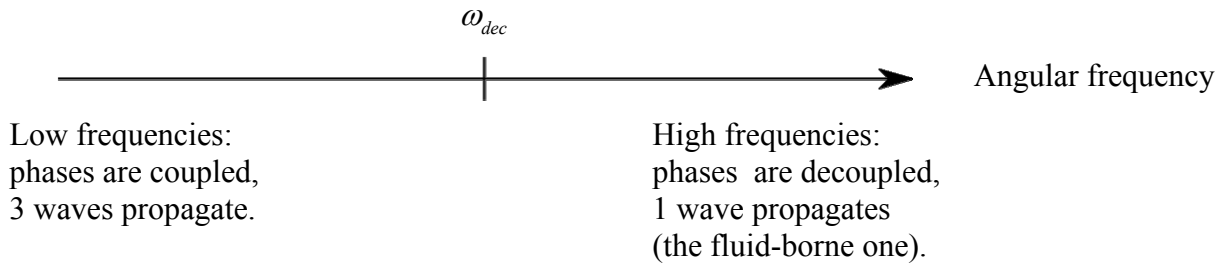

Figure 3. Frequency- dependent structural dissipation mechanisms

B. Conditions for a metal foam to be an acoustic absorber

To summarize the points above, two conditions on the pore network morphology can be stated for a metal foam to be an acoustic absorber:

1. An interconnected pore network for the dissipation mechanisms to occur in the largest possible volume.

2. Visco-inertial and thermal dissipation effects will significantly affect the sound wave propagation when the pores have a size of the same order of magnitude as that of the viscous and the thermal boundary layers.

From the work by Kirchhoff [45 - 46] it is known that the boundary layer thickness in a cylindrical tube for a plane wave incidence assuming a laminar flow of the air particle, a no-slip condition and no temperature jump at the air-frame interface, can be calculated as $\delta_v = \sqrt{\eta / \rho_0 2\pi f}$ where η is the dynamic viscosity of the air (1.8×10^{-5} N.s.m^{-2} at a temperature of 20 ^{o}C and an atmospheric pressure of 101325 Pa), ρ_0 is the mass density of the air at rest (1.2 kg.m^{-3} for the same temperature and atmospheric pressure conditions) and f is the frequency of the incident sound wave.

A quick numerical application leads to a variation of δ_v between 3.5×10^{-4} m and 1.1×10^{-5} m in the audible frequency range: [20 – 20 000] Hz.

Kirchhoff has also reported the expression of the thermal boundary layer thickness, for the same conditions as above: $\delta_t = \sqrt{\kappa / \rho_0 C_p 2\pi f}$ where κ is the thermal conductivity of air and C_p is its specific heat at constant pressure. For the same temperature and atmospheric pressure conditions as above, the numerical values of these two quantities are respectively 2.6×10^{-2} W.m^{-1}.K^{-1} and 1.0×10^{3} J.kg^{-1}.K^{-1}.Again, a quick numerical application leads to a variation of δ_t between 4.1×10^{-4} m and 1.3×10^{-5} m in the audible frequency range.From the simple physical analysis above on visco-inertial and thermal effects, it appears that the second condition for a metal foam to be an acoustic absorber, is to present a pore size in the approximate range [10 – 1000] micrometers.

Let us finally mention that efficient transmission losses are generally obtained with multilayered systems, where the poroelastic layer acts as a decoupling element. This is obviously not the case for metallic foams, which are too rigid to be attractive for this application. Consequently, metallic foams for sound insulation should be closed-cell, or used for their sound absorption properties.

Possible effects of altering the microstructure of a specific foam and the resulting acoustical properties to achieve optimal structural acoustic performance in a given application were discussed by Lind-Nordgren and Göransson recently [47].

III. Micro-macro simulation method

A. Metallic foams cellular morphology

Without exhaustivity objective, the intent of this section is to provide a brief overview of the diversity of microstructures which can be encountered when dealing with metallic foams and acoustic applications, together with possible corresponding periodic unit cell local geometry models; Fig. 4. Fig. 4(a) illustrates a 40 ppi Duocel® aluminum cylindrical foam sample mostly open cell. The foam sample diameter is 10 mm. The corresponding periodic unit cell foam model geometry is a regular truncated octahedra, also called tetrakaidecahedron, having ligaments of circular cross-section shapes. The reader is referred to Ref. 34 for a detailed study on this kind of foam sample microstructure and local geometry models. In Fig. 4(b), an initially closed cell aluminum foam sample is presented, showing cracks at the surface of the pores obtained by fracturing the cell walls via rolling. See Ref. 41 for more details about this technique used for improving sound absorbing properties of closed cell metallic foams. The related periodic unit cell is a simple body-centered cubic system with spheres allowed to interpenetrate in order to model interconnected openings. Fig. 4(c) presents a 22.6 mm thickness perforated metallic foam sample. Associated local geometry model is a simple cylinder with interconnected polydispersed spheres. See Ref. 27 for more information. It is also probably the place to underline the importance of collecting information on the fabrication process and related physics for modeling the typical cellular morphology of the metallic foam under interest. For an introduction of the different manufacturing routes for metallic foams, the reader is for instance referred to Ref. 48. Despite the variability of metallic foam's cellular morphology, a common question to be addressed by engineers and researchers interested in metallic foams' acoustic properties, and more specifically in bottom-

up approaches for improving their sound absorbing properties, might be formulated as the following. What are the local geometry parameters to be introduced in the micro-macro modeling of the porous media? i.e., pore size and interconnection distributions, property gradients and (an)isotropy. The answer to this question is not unique. But among the advantages to consider an idealized periodic unit cell reconstruction approach instead of addressing explicitly the disordered nature of porous media, are its effective ability to (i) grasp the main local geometry features having a significant impact at the upper scale as well as (ii) suitability for optimization purposes by means of a hybrid numerical approach. The work considered in this chapter leads to the determination of a periodic unit cell, from which macro-properties are derived. In particular, this method is illustrated through the case of a 40 ppi Duocel® aluminum foam sample as depicted in Fig. 4(a), for which an extensive literature exists on both microstructure and physical macro-behavior. In this application, reconstruction is carried out from the standpoint of the ligament length L and thickness t distributions, which have been acquired by means of X-ray computed axial microtomography [34]. A simple isotropic three-dimensional model is considered for the representative idealized periodic unit cell, with ligaments of circular cross-section shapes, and spherical nodes at their intersections (of diameter $d = 1.5 \times t$ typical of lump modeling).

The open porosity ϕ of a porous solid is defined as the fraction of the interconnected pore fluid volume Ω_f to the total bulk volume of the porous aggregate Ω,

$$\phi = \Omega_f / \Omega . \tag{1}$$

The thermal characteristic length Λ', which is a generalization of the hydraulic radius, is equal to twice the interconnected pore fluid volume Ω_f to pore wet surface $\partial\Omega$ ratio,

$$\Lambda' = 2\ \Omega_f / \partial\Omega . \tag{2}$$

The purely geometrical macroscopic properties – open porosity and thermal characteristic length of the idealized reconstructed PUC, might then be determined by spatial integration and compared with experimental measurements, with a view to validating the proposed idealized PUC prior to

first principles computations of transport properties. It is worth mentioning that the studied thermal characteristic length – commonly used in acoustics of porous media – is a parameter closely related to the specific surface of the solid porous frame [49].

Here, we do not use the mean values as input parameters for L and t. Instead, values corresponding to the main peaks of the modal distributions are considered ("mean1" in the notations of Ref. 34): L = 1000 μm and t = 330 μm.

B. Hybrid numerical approach

1. First principles calculations of transport properties

Previous studies [14, 50] have shown how the long-wavelengths acoustic properties of rigid-frame porous media can be numerically determined by solving the local equations governing the asymptotic frequency-dependent visco-thermal dissipation phenomena in a periodic unit cell with adequate boundary conditions. In the following, it is assumed that $\lambda >> D$, where λ is the wavelength of an incident acoustic plane wave. This means that for characteristic lengths on the order of $D \sim 0.5$ mm, this assumption is valid for frequencies reaching up to a few tens of kHz. The asymptotic macroscopic properties of sound absorbing materials are computed from the numerical solutions of:

(1) the low Reynolds number viscous flow equations (the static viscous permeability k_0, and the static viscous tortuosity α_0);

(2) the non-viscous flow or inertial equations (the high-frequency tortuosity α_∞, and Johnson's velocity weighted length's parameter Λ);

(3) the equations for thermal conduction (the static thermal permeability k_0', and the static thermal tortuosity α_0').

a) Viscous flow

At low frequencies or in a static regime, when $\omega \to 0$, viscous effects dominate, and the slow fluid motion in steady state regime created in the fluid phase Ω_f of a periodic porous medium having a unit cell Ω, is the solution of the following boundary value problem defined on Ω by [51]:

$$\eta \Delta \mathbf{v} - \nabla \mathsf{p} = -\mathsf{G}, \quad \text{in } \Omega_f, \tag{3}$$

$$\nabla . \mathbf{v} = 0, \quad \text{in } \Omega_f, \tag{4}$$

$$\mathbf{v} = 0, \quad \text{on } \partial\Omega, \tag{5}$$

$$\mathbf{v} \text{ and } \mathsf{p} \text{ are } \Omega\text{-periodic}, \tag{6}$$

where $\mathsf{G} = \nabla \mathsf{p}^m$ is a macroscopic pressure gradient acting as a source term, η is the viscosity of the fluid, and $\partial\Omega$ is the fluid-solid interface. This is a steady Stokes problem for periodic structures, where $\mathbf{v}$ is the Ω-periodic velocity, p is the Ω-periodic part of the pressure fields in the pore verifying $\langle \mathsf{p} \rangle = 0$, and the symbol $\langle\ \rangle$ indicates a fluid-phase average. It can be shown that the components v_i of the local velocity field are given by

$$v_i = -\frac{k_{0ij}^*}{\eta} G_j . \tag{7}$$

The components of the static viscous permeability tensor are then given by [15, 52]

$$k_{0ij} = \phi \langle k_{0ij}^* \rangle . \tag{8}$$

And the components of the tortuosity tensor are obtained from

$$\alpha_{0ij} = \langle k_{0\,pi}^* k_{0\,pj}^* \rangle / \langle k_{0\,ii}^* \rangle \langle k_{0\,jj}^* \rangle , \tag{9}$$

wherein the Einstein summation notation on p is implicit. In the present work, the symmetry properties of the microstructure under consideration imply that the second order tensors $\mathbf{k}_0$ and $\boldsymbol{\alpha}_0$ are isotropic. Thus $k_{0ij} = k_0 \delta_{ij}$ and $\alpha_{0ij} = \alpha_0 \delta_{ij}$, where δ_{ij} is the Kronecker symbol.

b) Inertial flow

At the opposite frequency range, when ω is large enough, the viscous boundary layer becomes negligible and the fluid tends to behave as a perfect one, having no viscosity except in a boundary layer. In these conditions, the perfect incompressible fluid formally behaves according to the problem of electric conduction [21, 53, 54], i.e. :

$$\mathbf{E} = -\nabla\varphi + \mathbf{e}, \quad \text{in } \Omega_f, \tag{10}$$

$$\nabla \cdot \mathbf{E} = 0, \quad \text{in } \Omega_f, \tag{11}$$

$$\mathbf{E} \cdot \mathbf{n} = 0, \quad \text{on } \partial\Omega, \tag{12}$$

$$\varphi \text{ is } \Omega\text{-periodic}, \tag{13}$$

where $\mathbf{e}$ is a given macroscopic electric field, $\mathbf{E}$ the solution of the boundary problem having $-\nabla\varphi$ as a fluctuating part, and $\mathbf{n}$ is unit normal vector to the boundary of the pore region.

Then, the components $\alpha_{\infty ij}$ of the high frequency tortuosity tensor can be obtained from [14]

$$e_i = \alpha_{\infty ij} \left\langle E_j \right\rangle. \tag{14}$$

In the case of isotropy, the components of the tensor $\boldsymbol{\alpha}_\infty$ reduce to the diagonal form $\alpha_{\infty ij} = \alpha_\infty \delta_{ij}$. In this case, the tortuosity can also be obtained from the computation of the mean square value of the local velocity through:

$$\alpha_\infty = \frac{\left\langle \mathbf{E}^2 \right\rangle}{\left\langle \mathbf{E} \right\rangle^2}. \tag{15}$$

As for the low frequency tortuosity, an extended formula can be used for anisotropic porous media. Having solved the cell conduction problem, the viscous characteristic length Λ can also be determined (for an isotropic medium) [6]

$$\Lambda = 2\frac{\int_\Omega \mathbf{E}^2 \, dV}{\int_{\partial\Omega} \mathbf{E}^2 \, dS}. \tag{16}$$

c) Thermal effect

When a vibration occurs, the pressure fluctuation induces a temperature fluctuation inside the fluid, due to the constitutive equation of a thermally conducting fluid. If one considers the solid frame as a thermostat, it can be shown that the mean excess temperature in the air $\langle \tau \rangle$ is proportional to the mean time derivative of the pressure $\partial \langle p \rangle / \partial t$. This thermal effect is described by $\langle \tau \rangle = (k_0' / \kappa) \partial \langle p \rangle / \partial t$, where $\langle \tau \rangle$ is the macroscopic excess temperature in air, κ is the coefficient of thermal conduction, and k_0' is a constant. The constant k_0' is often referred to as the "static thermal permeability". As the usual permeability, it has the dimensions of area and was named by Lafarge *et al.* [13]. It is related to the "trapping constant" Γ of the frame by $k_0' = 1/\Gamma$ [54]. In the context of diffusion-controlled reactions, it was demonstrated by Rubinstein and Torquato [55] that the trapping constant is related to the mean value of a "scaled concentration field" $u(\mathbf{r})$ by

$$\Gamma = 1 / \langle u \rangle , \tag{17}$$

where $u(\mathbf{r})$ solves

$$\Delta u = -1 , \quad \text{in } \Omega_f , \tag{18}$$

$$u = 0 , \quad \text{on } \partial\Omega . \tag{19}$$

It is worthwhile noticing that Δu is dimensionless. Therefore, u and k'_0 have the dimension of area. Similar to the tortuosity factors obtained from viscous and inertial boundary value problems, a "static thermal tortuosity" is given by :

$$\alpha_0' = \frac{\langle u^2 \rangle}{\langle u \rangle^2} . \tag{20}$$

2. Estimates of the frequency dependent visco-inertial and thermal responses

The acoustic response of foams depends on the dynamic viscous permeability and the "dynamic thermal permeability". Both of these parameters could be obtained from dynamic FEM computations as in Ref. 23. The approach presented here relies on the fact that the finite element computations presented previously are easy to implement, and provide the asymptotic behavior for both dynamic "permeabilities". This asymptotic behavior constitutes the input data for the models which are used for predicting the full frequency range of the dynamic "permeabilities". Therefore the hybrid approach employed in our study makes use of the asymptotic parameters of the porous medium obtained by finite elements. Then, it will be possible to provide the dynamic permeabilities and to compare these values to experimental ones. In a first step, the three different models which are used to build the dynamic permeabilities from asymptotic parameters are briefly recalled.

Johnson *et al.* [8] and, later, Pride *et al.* [11] considered the problem of the response of a simple fluid moving through a rigid porous medium and subjected to a time harmonic pressure variation across the sample. In such systems they constructed simple models of the relevant response functions, the effective dynamic viscous permeability $\tilde{k}(\omega)$ or effective dynamic tortuosity $\tilde{\alpha}(\omega)$. The main ingredient to build these models is to account for the causality principle, and therefore for the Kramers-Kronig relations between real and imaginary parts of the frequency–dependent permeability. The parameters in these models are those which correctly match the frequency dependence of the first one or two leading terms of the exact results for the high- and low-frequency viscous and inertial behaviors.

Champoux and Allard [10] and thereafter Lafarge *et al.* [13, 14, 50], in adopting these ideas to thermally conducting fluids in porous media, derived similar relations for the frequency dependence of the so-called effective "dynamic thermal permeability" $\tilde{k}'(\omega)$ or effective dynamic compressibility $\tilde{\beta}(\omega)$, which varies from the isothermal to the adiabatic value when frequency

increases. The models for effective dynamic permeabilities were shown to agree with those calculated directly or independently measured. An important feature of this theory is that all of the parameters in the models can be calculated independently, most of them being, in addition, directly measurable in non acoustical experimental situations. In this regard, these models are very attractive because they avoid computing the solution of the full frequency range values of the effective permeabilities/susceptibilities. These models are recalled in Sec.III.B.3. They are based on simple analytic expressions in terms of well defined high- and low- frequency transport parameters which can be determined from first principles calculations [Sec. 1].

Such a hybrid approach was extensively used by Perrot, Chevillotte and Panneton in order to examine micro-/macro relations linking local geometry parameters to sound absorption properties for a two-dimensional hexagonal structure of solid fibers [24]. This method was recently completed by the use of easily obtained parameter (porosity ϕ and static viscous permeability k_0) of real foam samples, and by utilizing three-dimensional numerical computations [38].

As explicated, spatial integration provides the purely geometrical macroscopic parameters – the open porosity ϕ and the thermal characteristic length Λ'; and the five remaining input parameters for the models, α_0, α_∞, Λ, k_0', and α_0' can be obtained by means of first-principles calculations by appropriate field-averaging in the PUC (Fig. 4(a)).

Finally, the predictions of the three models for the effective dynamic permeabilities described in Sec.III.B.3 may be considered. In summary, the Johnson-Champoux-Allard" [JCA] model uses 5 parameters (ϕ, k_0, α_∞, Λ, Λ'), Johnson-Champoux-Allard-Lafarge" model [JCAL] uses in addition $k_0^{'}$, and Johnson-Champoux-Allard-Pride-Lafarge" [JCAPL] model uses the full set of parameters (ϕ, k_0, $k_0^{'}$, α_∞, Λ, Λ', α_0, and $\alpha_0^{'}$).

3. Models for motionless skeleton materials

To describe the macro-scale acoustic properties of rigid-frame air-saturated porous media, also called "equivalent fluid" by some authors, the knowledge of two complex response factors are

required. The dynamic tortuosity $\tilde{\alpha}_{ij}(\omega)$ is defined by analogy with the response of an ideal (non-viscous) fluid for which α_{ij} is real-valued and frequency independent,

$$\rho_0 \tilde{\alpha}_{ij}(\omega) \frac{\partial \langle \mathbf{v}_j \rangle}{\partial t} = -\mathbf{G}_j . \tag{21}$$

$\tilde{\alpha}_{ij}(\omega) = \tilde{\rho}_{ij}(\omega)/\rho_0$ is related to the dynamic viscous permeability by $\tilde{\alpha}_{ij}(\omega) = \nu\phi / i\omega\tilde{k}_{ij}(\omega)$. In these expressions, $\tilde{\rho}_{ij}(\omega)$ is the effective density of air in the pores, ρ_0 is the density of air at rest, and $\nu = \eta/\rho_0$ is the air kinematic viscosity.

Similarly, a compressibility effect is also observed at macro-scale in the acoustic response of a thermo-conducting fluid filled porous media, where a second convenient response factor is the normalized dynamic compressibility $\tilde{\beta}(\omega)$ which varies from the isothermal to the adiabatic value when frequency increases,

$$\frac{\tilde{\beta}(\omega)}{K_a} \frac{\partial \langle \mathrm{p} \rangle}{\partial t} = -\nabla \cdot \langle \mathbf{v} \rangle . \tag{22}$$

Here, $\tilde{\beta}(\omega) = K_a / \tilde{K}(\omega)$ is directly related to the dynamic (scalar) thermal permeability [13] by means of the relation $\tilde{\beta}(\omega) = \gamma - (\gamma - 1) i\omega\tilde{k}'(\omega)/\nu'\phi$. In these equations, $\tilde{K}(\omega)$ is the effective dynamic bulk modulus of air in the pores, $K_a = \gamma P_0$ is the air adiabatic bulk modulus, P_0 the atmospheric pressure, $\gamma = C_\mathrm{p}/C_\mathrm{v}$ is the specific heat ratio at constant temperature, $\nu' = \kappa/\rho_0 C_\mathrm{p}$, and C_p and C_v are the specific heat capacity at constant pressure and volume.

With a locally plane interface, having no fractal character, the long-wavelength frequency dependence of the visco-thermal response factors $\tilde{\alpha}_{ij}(\omega)$ and $\tilde{\beta}(\omega)$ have to respect definite and relatively universal behaviors, namely causality through the Kramers-Kronig relation [8, 54, 56] similar to models used for relaxation phenomena in dielectric properties. The equivalent dynamic tortuosity of the material and the equivalent dynamic compressibility of the material are $\tilde{\alpha}_{eq\,ij}(\omega) = \tilde{\alpha}_{ij}(\omega)/\phi$ and $\tilde{\beta}_{eq}(\omega) = \phi\tilde{\beta}(\omega)$.

Simple analytic admissible functions for the fluid phase effective properties for *isotropic* porous media respecting the causality conditions are

$$\tilde{\alpha}(\omega)=\alpha_\infty\left[1-\frac{1}{i\varpi}f(\varpi)\right],\qquad \tilde{\beta}(\omega)=\gamma-(\gamma-1)\left[1-\frac{1}{i\varpi'}f'(\varpi')\right]^{-1},\tag{23}$$

where f and f' are form functions defined by

$$f(\varpi)=1-P+P\sqrt{1+\frac{M}{2P^2}i\varpi},\qquad f'(\varpi')=1-P'+P'\sqrt{1+\frac{M'}{2P'^2}i\varpi'},\tag{24}$$

and ϖ and ϖ' are dimensionless viscous and thermal angular frequencies given by the following expressions,

$$\varpi=\frac{\omega}{\nu}\frac{k_0\alpha_\infty}{\phi},\qquad \varpi'=\frac{\omega}{\nu'}\frac{k_0'}{\phi}.\tag{25}$$

The quantities M, M', P and P' are dimensionless shape factors,

$$M=\frac{8k_0\alpha_\infty}{\Lambda^2\phi},\qquad M'=\frac{8k_0'}{\Lambda'^2\phi},\qquad P=\frac{M}{4\left(\frac{\alpha_0}{\alpha_\infty}-1\right)},\qquad P'=\frac{M'}{4\left(\alpha_0'-1\right)}.\tag{26}$$

- For $M'=P=P'=1$, $k_0'=\phi\Lambda'^2/8$), the dynamic visco-inertial and thermal response functions reduce to 5 parameters (ϕ, k_0, α_∞, Λ, Λ') named throughout the paper as "Johnson-Champoux-Allard" [JCA] model.
- When the requirement $k_0'=\phi\Lambda'^2/8$ is not fulfilled, k_0' must be explicitly taken into account, this is the 6 parameters "Johnson-Champoux-Allard-Lafarge" [JCAL] model, where M' may differ from unity.
- A complete model relies on 8 parameters (ϕ, k_0, k_0', α_∞, Λ, Λ', α_0, and α_0') and correctly matches the frequency dependence of the first two leading terms of the exact result for both high and low frequencies. This is the refined "Johnson-Champoux-Allard-Pride-Lafarge" [JCAPL] model.

Looking for plane waves solutions varying as $\exp[i(\omega t-\tilde{q}x)]$, Eqs. (21) and (22) yield the

equivalent dynamic wave number $\tilde{q}_{eq}(\omega)$ of the material and equivalent characteristic impedance $\tilde{Z}_{eq}(\omega)$ of the material

$$\tilde{q}_{eq} = \omega\left(\tilde{\alpha}_{eq}(\omega)\tilde{\beta}_{eq}(\omega)\frac{\rho_0}{K_a}\right)^{\frac{1}{2}}, \qquad \tilde{Z}_{eq} = \left(\frac{\tilde{\alpha}_{eq}(\omega)}{\tilde{\beta}_{eq}(\omega)}\rho_0 K_a\right)^{\frac{1}{2}}. \tag{27}$$

Thus, $\tilde{\alpha}_{eq}(\omega)$ and $\tilde{\beta}_{eq}(\omega)$ provide all pertinent information on the propagation and dissipation phenomena in the equivalent homogeneous material. Assuming an absorbing porous layer of thickness L_s that is backed by a rigid wall, the normal incidence sound absorption coefficient is

$$A_n = 1 - \left|\frac{\tilde{Z}_{sn} - 1}{\tilde{Z}_{sn} + 1}\right|^2, \tag{28}$$

with the normalized surface impedance of the porous medium defined as

$$\tilde{Z}_{sn} = \frac{\tilde{Z}_{eq}}{\rho_0 c_0}\coth\left(i\tilde{q}_{eq}L_s\right), \tag{29}$$

where c_0 is the sound speed in air.

IV. Results and discussion

A. Experimental validations

Transport parameters and normal incidence sound absorbing behavior were derived on the basis of an idealized reconstructed PUC as described through Sec. III A with the computational method presented in Sec. III B. See Tab. I and Fig. 5 for the corresponding numerical results, and their experimental counterparts, as obtained by the techniques and methods exhaustively described below. These results validate our approach. Also shown is a typical perforated closed-cell metallic foam sound absorption spectrum, Fig. 6. See Ref. 27 for a detailed presentation of these results. Note that, contrary to open cell foam samples, perforated closed cell metallic foam samples as well as perforated plates present selective (as opposed to large frequency bands) sound absorption

spectrums. A subsequent step consists in numerical experiments to provide insight about microstructure effects on acoustical macro-behavior.

The absorption performances of acoustical materials are usually measured in diffuse sound field according to ISO 354 (Acoustics – Measurement of sound absorption in a reverberation room). However, due to the small sample size of metallic foams usually available their sound absorption properties are usually measured for plane waves at normal incidence according to ISO 10534 (Determination of sound absorption coefficient and impedance in impedance tubes). Either method 1 or 2 of this latter standard test can be used.

Measurement of the sound absorption in normal incidence using an impedance tube [57] (cf. Fig. 7) can also be advantageous to carry out the estimations of 4 parameters introduced previously [58, 59]: the high-frequency limit of the tortuosity, the viscous and thermal characteristic lengths and the static thermal permeability.

The two remaining parameters of the JCAL model can be directly measured: (i) the static permeability was obtained by means of accurate measurements of differential pressures across serial mounted calibrated and unknown flow resistances, with a controlled steady and non-pulsating laminar volumetric air flow as described by Stinson and Daigle [60] and recommended in the corresponding standard ISO 9053 (method A) or ASTM C522 (cf. Fig. 8); (ii) and the open-porosity using methods such as those described by Champoux *et al.* [10] based on a previous work by Beranek [61] (cf. Fig. 9), Leclaire *et al.*[62], or Panneton *et al.* [63, 64].

A direct measurement of the high frequency limit of the tortuosity α_∞ has been presented by Brown [53]. The method based on the measurement of the electrical conductivity of the porous material requires the material's frame to be saturated with a conducting fluid and can only be applied to materials for which the frame is composed with a dielectric material (i.e. it does not conduct electricity). As an alternative to direct measurement or estimation from impedance tube measurements, ultrasonic methods also exist. Allard *et al.* [65] have proposed a method to estimate α_∞ from the increase of flight time and the damping of an ultrasonic pulse, when a material sample

is placed in between two ultrasonic transducers. From this work and in particular works by Johnson *et al.* [66] and Nagy [67], Leclaire *et al.* [68] have proposed a method to estimate α_∞, Λ, Λ' using ultrasonic transmission measurements with the same porous material frame saturated successively with two different gases (usually air and helium). Recently, Groby *et al.* [69] have adapted the works by Panneton and Olny [58] and Olny and Panneton [59] to estimate the four 4 last parameters of the JCAL model in the ultrasound domain from measurements of the transmitted and the reflected coefficients.

B. Numerical experiments: Microstructure effects on acoustical macro-behavior

Two main cellular morphology parameters were found to dominate the effects on acoustical macro-behavior of rigid porous media [24, 26, 27, 30]. It is worth mentioning that conclusions found by these authors on the basis of a simple two-dimensional lattice of hexagonal solid fibers [24, 26, 30], were confirmed for other kinds of metallic foams apparently very different [27] such as the closed cell perforated metallic foam sample system as illustrated by Fig. 4(c). These conclusions might thus be considered as general acoustical micro-macro relationships. They report the existence of an emerging knowledge in which key local geometry features, having a significant impact on the *long-wavelength* acoustical macro-behavior of *motionless* porous media in general and metallic foams in particular, might be isolated from the standpoint of idealized periodic unit cells.

The throat size, which might be defined as the smallest aperture in a regular array of interconnected pores, appears as being the most important local geometry parameters in terms of acoustical macro-behavior. For instance, the throat size is the distance between two solid inclusions if one considers a regular array of solid fibers; it becomes the diameter of perforations when one deals with a perforated closed cell metallic foam sample. Numerical experiments have shown that the throat size directly controls the static viscous permeability k_0 (or the resistivity σ, since $k_0 = \eta / \sigma$) of the porous media and, as a consequence, the overall level of sound absorption

(mainly by viscous dissipation mechanisms). In other words, if the aperture by which the compressional sound wave is allowed to penetrate is too small, reflection occurs and the sound wave can neither propagate, nor dissipate. By contrast, if the aperture is too large, the viscous boundary layer interacts only with a small fraction of the possible surface by which viscous interactions develop. In between there must exist an optimal opening zone, which was already known by Kirchhoff for pores of cylindrical cross-section shapes (Sec. II A 1), and might be estimated by the proposed approach for real metallic foam samples.

The second microstructural parameter revealed from numerical experiments as having a significant and direct impact on the acoustical macro-behavior is the pore size. For instance, twice the inter-fiber distance in case of a hexagonal lattice of solid fibers ($2l$ in the notations of Fig. 1 in Ref. 26); the characteristic bubble size when one considers perforated closed cell metallic foams (a in the notations of Fig. 2 in Ref. 27). Pore size effect can be interpreted in terms of sound absorption modulation of the main peak: the overall sound absorption level is essentially unchanged by the pore size at constant throat size, whereas the frequency at which maximum absorption occurs might be advantageously modified according to the knowledge of a noise source spectrum. This is another fruitful property for sound absorbers design. The phenomenological reasons behind this micro-macro pore-size/modulation-spectrum linkage might be described in terms of tortuosity: pore size increases with the infinite tortuosity factor α_∞, which tends to lower the frequency of the sound absorption peak.

V. Further remarks on the evaluation of acoustic properties of metal foams

To summarize, we have presented a general approach for linking scales in acoustics of porous media in which the acoustic properties computation of various three-dimensional metallic foam microstructures can be considered in a unified framework. Comparison with experiments yields very good agreements. This paves the road for a systematic microstructure optimization of

real sound absorbing materials. The transport and acoustic properties dependence of the local geometry model to membrane, anisotropy, and polydispersity effects will be published elsewhere.

References

[1] F. Han, G. Seiffert, Y. Zhao, and B. Gibbs, Acoustic absorption behaviour of an open-celled aluminium foam, J. Phys. D: Appl. Phys. 36, 294–302 (2003).

[2] Z. Xie, T. Ikeda, Y. Okuda, and H. Nakajima, Sound absorption characteristics of lotus-type porous copper fabricated by unidirectional solidification, Materials Science and Engineering A 386, 390–395 (2004).

[3] M. Hakamada, T. Kuromura, Y. Chen, H. Kusuda, and M. Mabuchi, Sound absorption characteristics of porous aluminum fabricated by spacer method, J. Appl. Phys. 100, 114908 (2006).

[4] M. Hakamada, T. Kuromura, Y. Chen, H. Kusuda, and M. Mabuchi, High sound absorption of porous aluminum fabricated by spacer method, Appl. Phys. Lett. 88, 254106 (2006).

[5] W. Pannert, R. Winkler, and M. Merkel, On the acoustical properties of metallic hollow sphere structures (MHSS), Materials Letters 63, 1121–1124 (2009).

[6] M. A. Biot, Theory of propagation of elastic waves in a fluid-saturated porous solid. I. Low frequency range, J. Acoust. Soc. Am., 28 (2) 168-178 (1956).

[7] M. A. Biot, Theory of propagation of elastic waves in a fluid-saturated porous solid. II. Higher frequency range", J. Acoust. Soc. Am. 28 (2), 179-191 (1956).

[8] D. L. Johnson, J. Koplik, R. Dashen, Theory of dynamic permeability and tortuosity in fluid-saturated porous media, J. Fluid Mech. Vol. **176**, 379 (1987).

[9] C. Boutin and J.-L. Auriault, Dynamic behavior of porous media saturated by a viscoelastic fluid: Application to bituminous concretes, Int. J. Eng. Sci. 28, 1157-1181 (1990).

[10] Y. Champoux, J. F. Allard, Dynamic tortuosity and bulk modulus in air-saturated porous media, J. Appl. Phys. **70**, 1975 (1991).

[11] S. R. Pride, F. D. Morgan, and A. F. Gangi, Drag forces of porous media acoustics, Phys. Rev. B **47**, 4964 (1993).

[12] D. Keith Wilson, Relaxation-matched modeling of propagation through porous media including fractal pore structure, J. Acoust. Soc. Am. 94, 1136-1145 (1993).

[13] D. Lafarge, *P. Lemarinier, J. F. Allard, V. Tarnow, Dynamic compressibility of air in porous structures at audib*le frequencies, J. Acoust. Soc. Am. **102**, 1995 (1997).

[14] D. Lafarge, The equivalent fluid model (Chapter 6, Part II) in *Materials and Acoustics Handbook*, Edited by C. Potel and M. Bruneau (Wiley, Chichester, 2009) pp 167-201.

[15] C. Boutin, C. Geindreau, Periodic homogenization and consistent estimates of transport parameters through sphere and polyhedron packings in the whole porosity range, Phys. Rev. E **82**, 036313 (2010).

[16] A. Craggs and J. G. Hildebrandt, Effective densities and resistivities for acoustic propagation in narrow tubes, J. Sound Vibrat. 92, 321-331 (1984).

[17] M. Y. Zhou, P. Sheng, First-principles calculations of dynamic permeability in porous media, Phys. Rev. B **39**, 12027 (1989).

[18] A. M. Chapman and J. J. L. Higdon, Oscillatory Stokes flow in periodic porous media, Phys. Fluids A 4, 2099-2116 (1992).

[19] M. Firdaouss, J. -L Guermond, and D. Lafarge, Some remarks on the acoustic parameters of sharp-edged porous media, Int. J. Eng. Sci. 36 (9), 1035-46 (1998).

[20] A. Cortis and D. M. J. Smeulders, On the viscous length scale of wedge-shaped porous media, Int. J. Eng. Sci. 39(8) 951-962 (2001).

[21] A. Cortis, D. M. J. Smeulders, J.-L. Guermond, and D. Lafarge, Influence of pore roughness on high-frequency permeability, Phys. Fluids 15 (6), 1766-75 (2003).

[22] A. Cortis, D. M. L. Smeulders, D .Lafarge, M. Firdaouss, and J.-L. Guermond, in IUTAM Symposium on Theoretical and Numerical Methods in Continuum Mechanics of Porous Materials. Series: Solid Mechanics and Its Applications, edited by W. Ehlers (Kluwer Academic Publishers, Held at the University of Stuttgart, Germany, 1999) pp. 187-192.

[23] S. Gasser, F. Paun, and Y. Brechet, Absorptive properties of rigid porous media: Application to face centered cubic sphere packing, J. Acoust. Soc. Am. 117, 2090-2099 (2005).

[24] C. Perrot, F. Chevillotte, and R. Panneton, Dynamic viscous permeability of an open-cell aluminum foam: computations vs experiments, J. Appl. Phys. 103, 024909 (2008).

[25] K. Schladitz, S. Peters, D. Reinel-Bitzer, A. Wiegmann, and J. Ohser, "Design of acoustic trim based on geometric modeling and flow simulation for non-woven, " Comp. Mater. Sci. 38, 56-66 (2006).

[26] C. Perrot, F. Chevillotte, and R. Panneton, Bottom-up approach for microstructure optimization of sound absorbing materials, J. Acoust. Soc. Am. 124, 940 (2008).

[27] F. Chevillotte, C. Perrot, and R. Panneton, Microstructure based model for sound absorption predictions of perforated closed-cell metallic foams, J Acoust Soc Am. 128, 1766-1776 (2010).

[28] C.-Y. Lee, M. J. Leamy, and J. H. Nadler, Acoustic absorption calculation in irreducible porous media: A unified computational approach, J. Acoust. Soc. Am. 126, 1862 (2009).

[29] C.-Y. Lee, M. J. Leamy, and J. H. Nadler, Frequency band structure and absorption predictions for multi-periodic acoustic composites, J. Sound Vibrat. 329, 1809-1822 (2010).

[30] C. Perrot, F. Chevillotte, R. Panneton, J.-F. Allard, and D. Lafarge, On the dynamic viscous permeability tensor symmetry, J. Acoust. Soc. Am. **124** EL210 (2008).

[31] D. Lafarge, *in Poromechanics II: Proceedings of the Second Biot Conference on Poromechanics*, edited by J. -L Auriault, 703-708 (Swets & Zeitlinger, Grenoble, 2002).

[32] S. Torquato, Efficient simulation technique to compute properties of heterogeneous media, Appl. Phys. Lett. **55** (18), 1847-1849 (1989)

[33] D. A. Coker and S. Torquato, Simulation of diffusion and trapping in digitized heterogeneous media, J. Appl. Phys. **77**, 955-964 (1994).

[34] C. Perrot, R. Panneton, and X. Olny, Periodic unit cell reconstruction of porous media: Application to an open cell aluminum foam, J. Appl. Phys. **101**, 113538 (2007).

[35] C. Perrot, R. Panneton, and X. Olny, Computation of the dynamic thermal dissipation properties of porous media by Brownian motion simulation: Application to an open-cell aluminum foam, J. Appl. Phys. **102**, 074917 (2007).

[36] X. Wang and T. J. Lu, Optimized acoustic properties of cellular solids, J. Acoust. Soc. Am. 106 (2), 756-765 (1999).

[37] I. Malinouskaya, V. V. Mourzenko, J.-F. Thovert, and P. M. Adler, Wave propagation through saturated porous media, 77, Phys. Rev. E **77**, 066302 (2008).

[38] C. Perrot, F. Chevillotte, G. Bonnet, F.-X. Bécot, M. T. Hoang, L. Gautron, and A. Duval, Microstructure, transport, and acoustic properties of open-cell foam samples: Experiments and three-dimensional numerical simulations, submitted to J. Appl. Phys. (02/2011).

[39] T. Miyoshi, M. Itoh, S. Akiyama, and A. Kitahara, Alporas aluminum foam: Production process, properties, and applications, Adv. Eng. Mat. **2** (4), 179-183 (2000).

[40] T. J. Lu, F. Chen, and D. He, Sound absorption of cellular metals with semiopen cells, J. Acoust. Soc. Am. 108 (4), 1697-1709 (2000).

[41] T. J. Lu, A. Hess, and M F. Ashby, Sound absorption in metallic foams, J. Appl. Phys. 85 (11), 7528-7539 (1999).

[42] Z. Xie, T. Ikeda, Y. Okuda, and H. Nakajima, Sound absorption characteristics of lotus-type porous copper fabricated by unidirectional solidification, Mat. Sci. and Eng. A 386, 390-395 (2004).

[43] C. Zwikker and C. W. Kosten, *Sound absorbing materials* (Elsevier, Amsterdam, 1949).

[44] J. F. Allard and N. Atalla, *Propagation of Sound in Porous Media: modeling sound absorbing materials*, 2nd Ed. (Wiley, Chichester, 2009).

[45] G. Kirchhoff, Ueber den Einfluss der Wärmeleitung in einem Gase auf die Schallbewegung, Ann. Phys. Chem. **134**, 177-193 (1868).

[46] G. Kirchhoff, On the influence of heat conduction in a gas on sound propagation, edited by R. B. Lindsay (Hutchidon & Ross, Dowden, 1974).

[47] E. Lind-Nordgren and P. Göransson, Optimising open porous foam for acoustical and vibrational performance, J. Sound Vibrat. **329**(7), 753-767 (2010).

[48] J. Banhart, Manufacturing Routes for Metallic Foams, Journal of Metals **52**, 22 (2000).

[49] Henry M, Lemarinier P, Allard JF, Bonardet JL, and Gedeon A. Evaluation of the characteristic dimensions for porous sound-absorbing materials. J. Appl. Phys. 1995; 77(1): 17-20 (1995).

[50] D. Lafarge, Comments on “Rigorous link between fluid permeability, conductivity, and relaxation times for transport in porous media”, Phys. Fluids A **5**, 500 (1993).

[51] J.-L. Auriault, C. Boutin and C. Geindreau, *Homogenization of coupled phenomena in heterogeneous media* (Wiley-ISTE, 2009).

[52] C. Boutin, C. Geindreau, Estimates and bounds of dynamic permeability of granular media, J. Acoust. Soc. Am. Vol. **124**, 3576 (2008).

[53] R. J. S. Brown, Connection between formation factor for electrical-resistivity and fluid-solid coupling factor in Biot equations for acoustic waves in fluid-filled porous media, Geophys. **45**, 1269 (1980).

[54] M. Avellaneda and S. Torquato, Rigorous link between fluid permeability, electrical conductivity, and relaxation times for transport in porous media, Phys. Fluids A 3, 2529 (1991).

[55] J. Rubinstein and S. Torquato, Diffusion-controlled reactions: Mathematical formulation, variational principles, and rigorous bounds, J. Chem. Phys. **88**, 6372 (1988).

[56] D. Lafarge, *Propagation du son dans les matériaux poreux à structure rigide saturés par un fluide viscothermique* (Ph. D. Thesis, Université du Maine, 1993); translation in English : " *Sound propagation in rigid porous media saturated by a viscothermal fluid* ".

[57] H. Utsuno, T. Tanaka, T. Fujikawa, A. F. Seybert, Transfer function method for measuring characteristic impedance and propagation constant of porous materials, J. Acoust. Soc. Am. **86**, 637 (1989).

[58] R. Panneton, X. Olny, Acoustical determination of the parameters governing viscous dissipation in porous media, J. Acoust. Soc. Am. **119**, 2027 (2006).

[59] X. Olny, R. Panneton, Acoustical determination of the parameters governing thermal dissipation in porous media, J. Acoust. Soc. Am. **123**, 814 (2008).

[60] M. R. Stinson and G. A. Daigle, Electronic system for the measurement of flow resistance, J. Acoust. Soc. Am. **83**, 2422 (1988).

[61] L. L. Beranek, Acoustic impedance of porous m**ate**rials, J. Acoust. Soc. Am. **13**, 248 (1942).

[62] P. Leclaire, O. Umnova, K. Horoshenkov and L. Maillet, Porosity measurement by comparison of air volumes, Rev. Sci. Instrum. 74(3), 1366-1370 (2003).

[63] R. Panneton and E. Gros, "A missing mass method to measure the open porosity of porous solids," Acta Acustica United With Acustica 91 (2), 342-8 (2005).

[64] Y. Salissou, R. Panneton, Wideband characterization of the complex wave number and characteristic impedance of sound absorbers, J. Acoust. Soc. Am. **128**, 2083-2090 (2010).

[65] J.-F. Allard, B. Castagnède, M. Henri and W. Lauriks, Evaluation of tortuosity in acoustic porous materials saturated by air, Rev. Sci. Instrum 65(3), 754-755 (1994).

[66] D. L. Johnson, T. J. Plona, C. Scala, F. Pasierb and H. Kojima, Tortuosity and acoustic slow waves, Phys Rev. Lett. 49, 1840-1844 (1982).

[67] P. B. Nagy, Slow wave propagation in air-filled permeable solids, J. Acoust. Soc. Am. 93, 3224-3234 (1993).

[68] P. Leclaire, L. Kelders, W. Lauriks, M. Melon, N. Brown and B. Castagnède, Determination of the viscous and thermal characteristic lengths of plastic foams by ultrasonic measurements in helium and air, J. Appl. Phys., 80 (4), 2009-2012 (1996).

[69] J.-P. Groby, E. Ogam, L. De Ryck, N. Sebaa and W. Lauriks, Analytical method for the ultrasonic characterization of homogeneous rigid porous materials from transmitted and reflected coefficients, J. Acoust. Soc. Am. 127(2), 764-772 (2010).

Table I Comparison between computed, measured, and characterized macroscopic parameters for a Duocel® 40 ppi aluminum foam sample.

Method	ϕ (-)	Λ' (mm)	k_0 (m^2)	α_0 (-)	Λ (μm)	α_∞ (-)	k_0' (m^2)	α_0'
Computations	0.91	2.05	10.34×10^{-8}	1.42	1.17	1.07	19.92×10^{-8}	1.21
Measurements [a, b]	0.91 (± 0.01)		10.39×10^{-8} ($\pm1.23\times10^{-8}$)					
Characterization [c, d]		2.01 (± 0.43)		NA	0.99 (± 0.06)	1.07 (± 0.01)	NA	NA

[a]References 63-64.
[b]Reference 60.
[c]Reference 59.
[d]Reference 58.

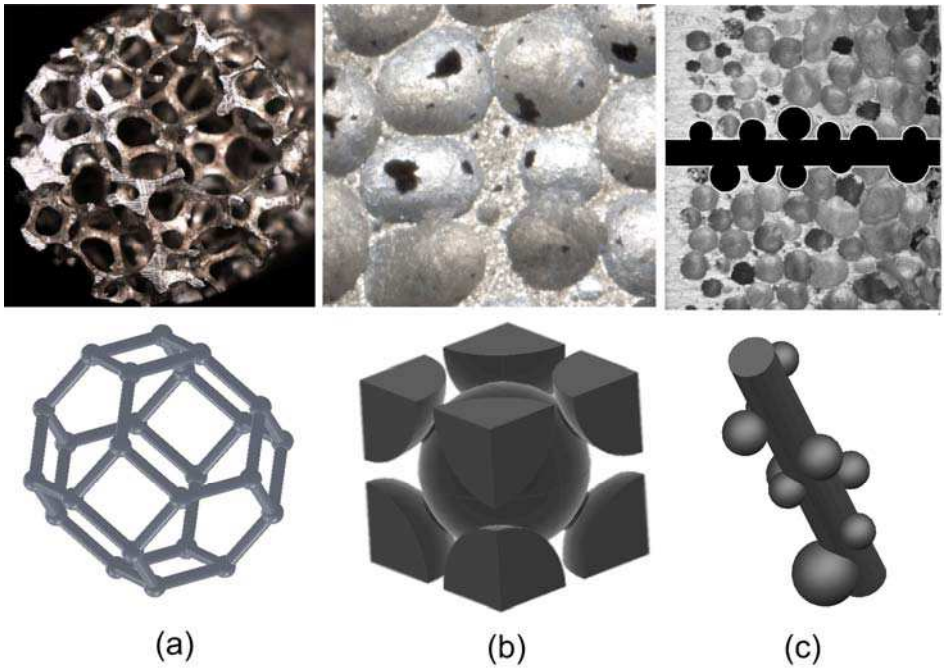

Figure 4. Illustration of the diversity of microstructures which can be encountered when dealing with metallic foams together with possible corresponding periodic unit cell local geometry models: (a) open cell, (b) fractured, and (c) perforated closed cell aluminum foam samples.

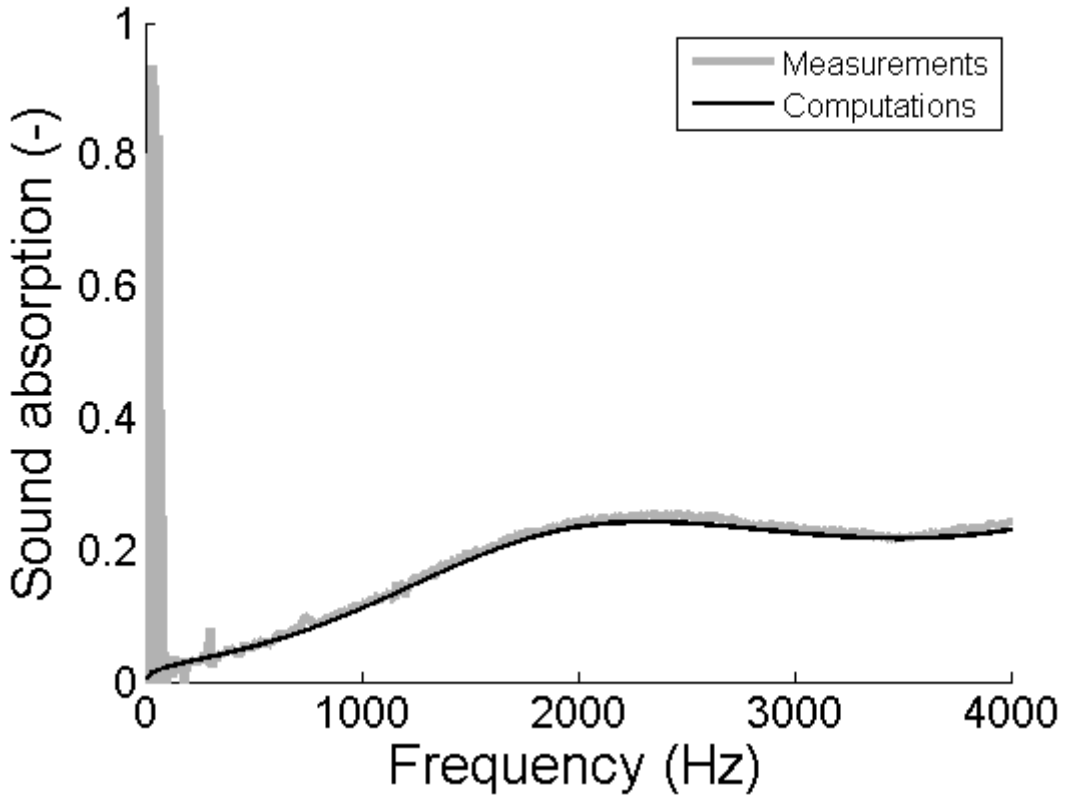

Figure 5. Comparison between computed and measured normal incidence, plane waves, sound absorbing behavior of a 40 ppi Duocel® aluminum foam sample. Thickness, 48 mm.

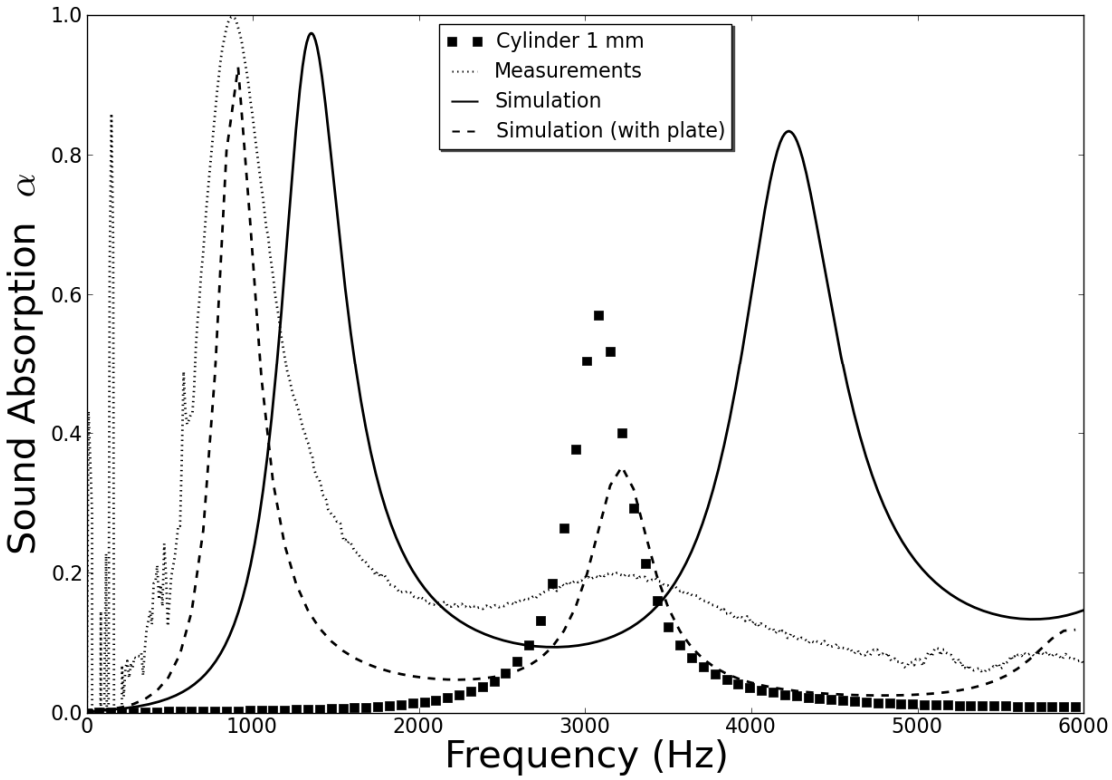

Figure 6. Normal incidence sound absorption coefficient of a real perforated closed-cell aluminum foam. Measurements (dotted line) compared to numerical computations with (dashed line) and without (solid line) a perforated facing plate.

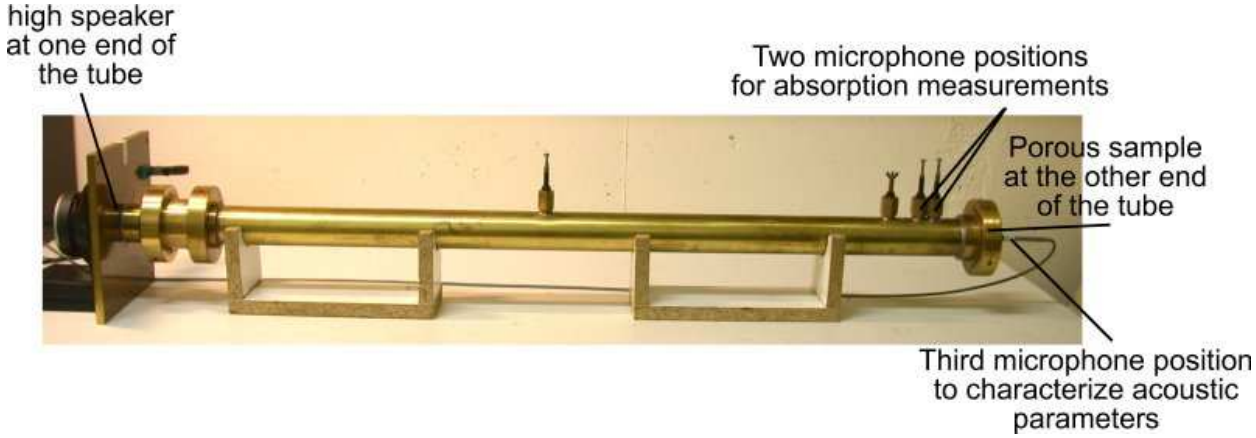

Figure 7. Picture of a 1 meter-long impedance tube which can be used (i) to measure the sound absorption properties of metal foams for plane waves at normal incidence and (ii) to estimate 4 parameters of the JCAL model.

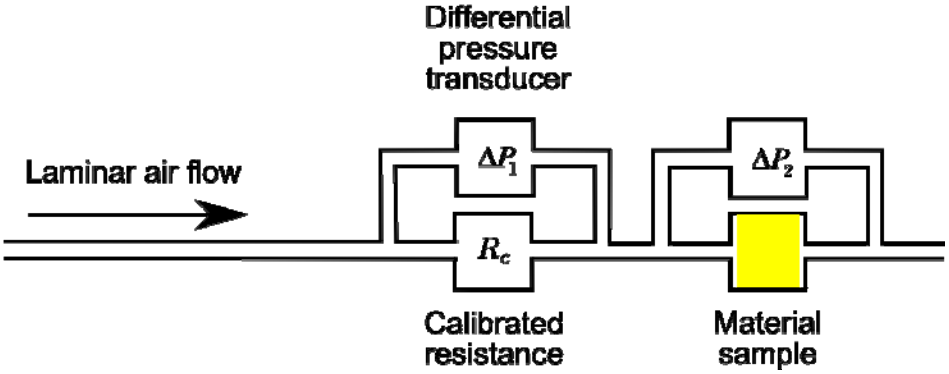

Figure 8. Scheme of the experimental setup used for the measurement of the static air flow resistivity.

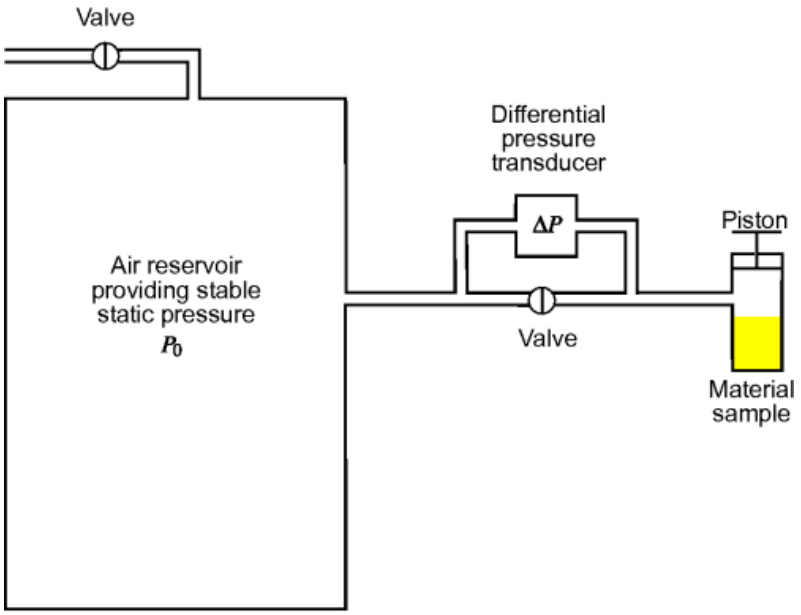

Figure 9. Scheme of the porosity measurement apparatus after Beranek [61] and Champoux *et al.* [10]. Porosity is measured from the pressure increase when reducing a reference volume containing the sample using Boyle-Mariotte law.